Monomer Exchange and Concentration Fluctuations of Micelles. Broad-Band Ultrasonic Spectrometry of the System Triethylene Glycol Monohexyl Ether/Water

T. Telgmann and U. Kaatze*

Drittes Physikalisches Institut, Georg-August-Universität, Bürgerstrasse 42-44, D-37073 Göttingen, Germany

Received: July 9, 1999; In Final Form: November 20, 1999

At four temperatures between 17.5 and 40 °C and several surfactant concentrations, the ultrasonic absorption spectra in the frequency range from 100 kHz to 2 GHz, the sound velocities, and the shear viscosities have been measured for aqueous solutions of triethylene glycol monohexyl ether. At solute concentrations smaller than or close to the critical micelle concentration (cmc), the broad-band spectra reveal one relaxation region reflecting the formation/decay kinetics of oligomeric species. The spectra of the more concentrated solutions show two different relaxations, one subject to a small the other to a broad distribution of relaxation times. The former relaxation is due to the monomer exchange between micelles and the suspending liquid. The parameters of this process largely follow the predictions of the Teubner−Kahlweit theory, which is based on the Aniansson−Wall model of micelle kinetics. Close to the cmc, however, the principal relaxation rate shows a different behavior, which is assumed to also result from the action of oligomeric species. The relaxation time distribution is considered a consequence of fluctuations in the local micelle concentration. The second relaxation, which extends over a significantly broader frequency range, can be well represented by the Bhattacharjee−Ferrell model of critical concentration fluctuations. For the solution of critical composition, the relaxation rates of local energy fluctuations derived from the ultrasonic spectra are confirmed by the (static) shear viscosity data. We discuss these fluctuations as to be due to variations in the local concentration of micelles.

1. Introduction

The formation and dynamics of supramolecular aggregates in binary liquid mixtures has been a topic of lively scientific debate for several years. Still today much interest is directed toward aggregation phenomena, particularly in view of many biophysical problems. Aqueous solutions of nonionic surfactants of the type $CH_3(CH_2)_{i-1}(OCH_2CH_2)_jOH$, for which the shorthand notation C_iE_j has become popular, offer favorable conditions for the study of different species of molecular structures. It is well-established that in C_iE_j/water systems, depending on the surfactant concentration, the temperature, and the particular composition of the poly(ethylene glycol)monoalkyl ether, micelles may be formed and that the mixtures may also possess a lower critical solution temperature. The kinetics of micelle formation is usually interpreted in terms of the Aniansson−Wall model.[1−5] In this model an isodesmic scheme of coupled chemical reactions

$$N_1 + N_{i-1} \underset{k_i^b}{\overset{k_i^f}{\rightleftharpoons}} N_i, \quad i = 2, ..., N \tag{1}$$

is assumed along with a reasonable size distribution of aggregates, presupposed to be nearly Gaussian for the micelle region. A somewhat refined distribution function has been proposed recently[6] to account for the particular behavior of solutions of amphiphiles with high critical micelle concentration (c_{cmc}). In eq 1 N_i denotes the concentration of aggregates consisting of i surfactant molecules while k_i^f and k_i^b are the forward and backward rate constants, respectively.

Near the critical demixing point, fluctuations with long-range correlations in the order parameter occur. The critical behavior of the C_iE_j/water mixtures seems to reveal two groups.[7] For one group, light scattering yields correlation length and generalized susceptibility data in conformity with the Landau−Wilson−Ginzburg renormalization group theory. For the other mixtures, both quantities exhibit critical exponents that are smaller than expected theoretically.[7] It has been suggested that this discrepancy follows from an incomplete consideration of noncritical contributions from micellar aggregates in the analysis of experimental data.

Initially there existed alternative ideas of the microdynamics in C_iE_j/water systems. However, the view by Corti and Degiorgio is now generally accepted that aqueous solutions of nonionic amphiphiles, at a lower critical solution temperature, may separate into a micelle-poor and a micelle-rich phase.[8] It has been suggested that such critical systems belong to the same universality class as ordinary (molecularly dispersed) nonionic binary liquid mixtures.[9] It is the aim of a series of papers on the microdynamics of C_iE_j/water systems to illuminate this view by results from ultrasonic spectrometry. An aspect of special interest is the effect of the critical phenomena on the kinetics of amphiphilic molecule exchange between the micelles and the suspending phase.

Ultrasonic spectrometry has proven a powerful tool for the study of the kinetics of micelle formation.[10−21] In conformity with theoretical predictions,[22,23] Debye-type relaxation spectra are found for proper micelle systems. In contrast, ultrasonic spectra resulting from concentration fluctuations in critical binary mixtures exhibit a characteristic shape,[24−32] reflecting a

10.1021/jp9923116 CCC: $19.00
Published on Web 01/25/2000

broad continuous distribution of relaxation times. Broad-band ultrasonic spectrometry is thus a suitable method for the investigation of the micelle kinetics and of the fluctuations in the local micelle concentration of nonionic surfactant solutions.

In this article we focus on the system C_6E_3/water. It exhibits a critical micelle concentration ($c_{cmc} = 0.1$ mol/L,[33] $Y_{cmc} = 0.02$, $Y =$ mass fraction of surfactant) and a lower critical demixing point ($c_{crit} = 0.6$ mol/L,[34] $Y_{crit} = 0.146$;[7] $T_{crit} = 44.7$ °C[34]), which are promising for spectroscopic measurements at different concentrations and temperatures. The system belongs to the aforementioned group of C_iE_j/water mixtures, the critical exponents of which follow the Landau−Wilson−Ginzburg model, e.g., $\tilde{\nu} = 0.63$ and $\gamma = 1.25$.[34] Here $\tilde{\nu}$ is the critical exponent of the correlation length

$$\xi(T) = \xi_0 t^{-\tilde{\nu}} \tag{2}$$

and γ that of generalized susceptibility

$$\chi_T(T) = \chi_{T,0} t^{-\gamma} \tag{3}$$

where $t = (T_{crit} - T)/T_{crit}$ denotes the reduced temperature. Among a variety of C_iE_j/H_2O and C_iE_j/D_2O systems C_6E_3/H_2O evidences a small amplitude of the correlation length ($\xi_0 = 0.35$ nm[7]).

Ultrasonic absorption spectra of C_6E_3/H_2O mixtures have been already measured between 3.96 and 11.65 MHz[35] and between 0.5 and 155 MHz,[36] respectively. These spectra have been discussed in terms of a single Debye-type relaxation process, assumed to be due to the kinetics of micelle formation. For more concentrated solutions, spectra between 5 and 160 MHz have been fitted to a double-Debye-term model and have also been associated to micellar exchange equilibria.[37] So far ultrasonic studies did not reveal any contributions from fluctuations in the micelle concentration.[35−37] On the basis of these results, the opinion has been expressed that the absence of critical contributions in the sonic spectra might reflect a characteristic feature of supramolecular binary mixtures, indicating a negligibly small coupling between the acoustical waves and the order parameter fluctuations.

In this situation it seemed to be interesting to us to look for contributions from concentration fluctuations in an extended frequency range of measurements. Here we report ultrasonic spectra between 100 kHz and 2 GHz, measured at four temperatures between 17.5 and 40 °C for C_6E_3/water mixtures of five different compositions.

2. Ultrasonic Spectrometry

General Aspects. The absorption coefficient α of acoustical waves in liquids is normally expressed by two terms

$$\alpha(\nu) = B'\nu^2 + \alpha_{exc}(\nu) \tag{4}$$

Herein, $B'\nu^2$ denotes a background contribution with B' independent of frequency ν. $\alpha_{exc}(\nu)$ is the frequency-dependent excess part in which we are interested. Because of the "classical" absorption, due to viscous friction and heat conductance,[38] a background contribution to $\alpha(\nu)$ is always present. However, B' may contain further contributions, for instance, from the volume viscosity. The background contribution is small at low frequencies but becomes the dominating term in eq 4 at high frequencies. For this reason resonator methods have been used in the lower frequency range ($\nu < 15$ MHz). When these methods are applied, the effect of the sample properties in the acoustical wave characteristics is significantly enhanced by multiple reflections. At high frequencies ($\nu > 1$ MHz), pulse-modulated propagating wave transmission techniques have been applied at variable sample thicknesses.

Fixed Path-Length Resonator Method. In the resonator measurements, the liquid sample was contained in either of two different circular cylindrically shaped cavities, the end faces of which were made of piezoelectric quartz disks. At a series of resonance frequencies ν_{rn}, $n = 1, 2, ...$, of the cell the α-value of the liquid was determined from the change in the quality factor Q of the cavity when the liquid was exchanged for a reference liquid of well-known absorption coefficient.[39] To meet the sample wavelength and the reflection coefficient at the liquid/transducer interfaces as close as possible, aqueous solutions of sodium chloride or methanol/water mixtures with carefully matched sound velocity and density have been used in the reference measurements at 25 °C. At the other temperatures of measurements, water has been used as reference, utilizing the sound velocity data according to Bilaniuk and Wong,[40] the density data as given by Kell,[41] and absorption coefficients as measured with the aid of the pulse-modulated wave transmission method. At 7 °C $\le T \le$ 40 °C, within an error of 2% the latter data can be represented by the polynomial

$$\alpha/\nu^2 = (51.71 - 1.997\mathrm{K}^{-1}T + 3.88 \times 10^{-2}K^{-2}T^2 - 3.05 \times 10^{-4}K^{-3}T^3) \times 10^{-15}\ \mathrm{s^2\ m^{-1}} \tag{5}$$

We used a biplanar resonator cell[42] in the upper frequency range (0.8 MHz $\le \nu \le$ 15 MHz; cell diameter $2R = 16.8$ mm, cell length $l = 6$ mm, fundamental frequency of transducer thickness vibrations $\nu_T = 4$ MHz). In the lower frequency range (0.1 MHz $\le \nu \le$ 2.7 MHz), to reduce the effect of diffraction, a plano-concave cell[43] was utilized ($2R = 70$ mm, $l = 19$ mm, $\nu_T = 1$ MHz, radius of curvature $R_c = 2$ m). To properly account for higher order cavity modes, we always recorded, in the frequency range around a primary resonance peak, the complex resonator transfer function, using a computer-controlled network analyzer (HP 4195A), and fitted suitable theoretical functions[44,45] to the spectrum. When these functions were applied, allowance was also made for cross-talk.

In addition to the sound velocity c_s and density ρ, the absorption coefficient of the reference should also agree as close as possible with that of the sample.[46] Because we were unable to also meet this condition, suitable corrections have been calculated to account for differences in the α-values.[46] For the present samples, however, the corrections turned out to be negligibly small throughout.

Variable Path-Length Pulse-Modulated Wave Transmission Method. At frequencies above 3 MHz, the attenuation coefficient of the samples has been measured by propagating a pulse-modulated wave of frequency ν through a cell of variable sample length z.[39] Possibly existing small instabilities and nonlinearities of the electronic apparatus were taken into account by periodical calibration procedures in which the sample cell was replaced by a high-precision below-cutoff piston attenuator with appropriately chosen relative attenuation increment.[47,48] Owing to the nonvanishing reflection coefficient r at the transmitter crystal/liquid and liquid/receiver crystal interfaces, standing wave patterns may also exist in excess to the propagating wave. In general, the amount of the receiver voltage $|U_r|$ is given by the expression

$$|U_r| = \left|U_0 \frac{(1 + r)\exp(-\gamma(z - z_0))}{1 - r^2\exp(-2\gamma(z - z_0))} + U_c \exp(i\Delta\phi_c)\right| \tag{6}$$

Herein $\gamma = \alpha + i\beta = \alpha + i2\pi/\lambda$, $\lambda = c_s/\nu$, denotes the complex propagation constant, z_0 considers a prospective small error in the zero-range setting of the distance meter, U_0 is an amplitude, and U_c and $\Delta\phi_c$ are the amplitude and phase difference of a contribution from electrical cross-talk. In most parts of the measuring frequency range, the pulsed mode of operation, owing to transit-time differences, allows for an effective separation of the multiple reflections and the electrical cross-talk as well. Equation 6 then reduces to the simple exponential

$$|U_r| = U_0 e^{-\alpha z} \tag{7}$$

Since the transducer area A is finite, diffraction effects may affect the cell transfer function at frequencies below 30 MHz. According to Menzel,[48,49] these effects can be taken into account by a semiempirical correction term, using the relation

$$|U_r| = U_0 e^{-\alpha z}[e^{(z\lambda/(2\pi A))^{1/2}}]^{g(z)} \tag{8}$$

with

$$g(z) = 1 - z/(0.1\ \text{m}) \tag{9}$$

We used four different cells to cover the frequency range. Up to about 500 MHz, three cells were available in which matched transmitter and receiver transducer disks were operated at the odd overtones of their fundamental frequency of thickness vibrations. The cells mainly differed in the parameters of the transducers (3 MHz $\le \nu \le$ 60 MHz, transducer diameter $2R_T$ = 40 mm, ν_T = 1 MHz, quartz;[48] 3 MHz $\le \nu \le$ 120 MHz, $2R_T$ = 60 mm, ν_T = 1 MHz, quartz;[50] 30 MHz $\le \nu \le$ 500 MHz, $2R_T$ = 12 mm, ν_T = 10 MHz, lithium niobate[51]). Between 0.5 and 2 GHz broad-band end-face excitation[52] of lithium niobate rods ($2r_T$ = 3 mm, length l_r = 10 mm[49,53] was utilized.

The sample length z was varied in a computer-controlled mode using stepping motor drives (up to 10^4 steps per turn) and was measured with the aid of optical grating distance meters.

Sound Velocity Measurements. In the lower part of the frequency range of measurements, the sound velocity c_s of the samples has been derived from the distances between series of resonance frequencies ν_{rn} of the cavity resonator cells using the relation[39,43]

$$c_s = 2\pi l(\nu_{rn} - \nu_{rn-1})/\arccos\left(\frac{(g_n^2 - 1)(1 - g_{n-1}^2) - 4g_n g_{n-1}}{(g_n^2 + 1)(g_{n-1}^2 + 1)}\right) \tag{10}$$

where

$$g_m = \frac{\rho c_s}{\rho_T c_T}\tan(\pi\nu_m/\nu_T), \quad m = 1, 2, \ldots \tag{11}$$

Herein ρ_T and c_T denote the transducer density and sound velocity, respectively. Equations 10 and 11 describe the non-equidistancy of the cell resonance frequencies ν_{rn} due to the incomplete reflection of the sonic waves at the liquid/transducer interfaces.

At higher frequencies c_s was derived from the waviness of the transfer function $|U_r(x)/U_0|$ of the cells (eq 6) due to multiple reflections of the sonic signal at small transducer spacing z.

Experimental Accuracy. Fluctuations in the measuring frequency were negligibly small. The temperature of the sample cells was controlled to within 0.02 K, and it was measured with an accuracy of 0.02 K. At room temperature, gradients and differences in the temperature of different cells thus did not exceed 0.04 K. At the other temperatures of measurement, the gradients may be somewhat stronger. Nevertheless, the effect of temperature fluctuations in the absorption coefficient data was small throughout.

Errors in the α-measurements with fixed path-length resonator cells predominantly result from an insufficient matching of the sound velocity and density of the reference liquid, from incomplete consideration of the spurious higher order modes for samples with high absorption coefficient, and from inperfect wetting of the cell surfaces, due to unfavorable surface tension conditions. In the lower frequency range (ν < 30 MHz), errors in the variable path-length pulse-modulated wave transmission measurements may result from the empirical correction for diffraction losses (eq 8). At higher frequencies (ν > 500 MHz), the limited resolution and accuracy of the high-precision distance meters is the dominating source of possible errors. Some of the samples reported here exhibit rather high absorption coefficients so that power levels higher than usual had to be applied.

As a result of various sources of error, the accuracy of the measurements depends on the properties of the samples themselves. The accuracy can be globally characterized by an uncertainty of $\Delta\alpha/\alpha = 0.05$ in the data resulting from resonator measurements. The error may be somewhat higher ($\Delta\alpha/\alpha$ = 0.1) at small α and at ν < 300 kHz. For the data from pulse-modulated wave transmission measurements $\Delta\alpha = 0.02$ at 3 MHz $\le \nu \le$ 50 MHz and $\Delta\alpha/\alpha = 0.01$ at 50 MHz $\le \nu \le$ 2 GHz.

The error in the sound velocity is $\Delta c_s/c_s = 0.001$ at ν < 3 MHz and at ν > 500 MHz, and it is $\Delta c_s/c_s = 0.0005$ at 3 MHz $\le \nu \le$ 500 MHz.

Least-Squares Regression Analysis of Measured Spectra. It is common practice to discuss ultrasonic absorption spectra in either format, α/ν^2 vs ν or $\alpha\lambda$ vs ν. The former shows the background contribution of the spectra as a frequency independent part B', which toward high frequencies is asymptotically approached by the data. The latter format, in which the background part contributes a term $B\nu$ to the spectrum ($B = B'c_s$), is more suitable for a comparison with theoretical models. To fit theoretical model relaxation spectral functions $R(\nu, P_j)$, corresponding with $\alpha\lambda = (\alpha\lambda)_{exc} + B\nu$ data, to the measured spectra we used a Marquardt algorithm[54] to minimize the variance

$$\chi^2 = \frac{1}{N - J - 1}\sum_{n=1}^{N}\left(\frac{(\alpha\lambda)_n - R(\nu_n, P_j)}{\Delta(\alpha\lambda)_n}\right)^2 \tag{12}$$

Here P_j, $j = 1, \ldots, J$, are the parameters of R and ν_n, $n = 1, \ldots, N$, are the frequencies of measurement. $(\alpha\lambda)_n$ and $\Delta(\alpha\lambda)_n$ denote the absorption per wavelength data and their experimental error, respectively, at ν_n. The use of weighting factors that are inversely proportional to the absolute experimental errors ($1/\Delta(\alpha\lambda)_n$ in eq 12) leads to the same parameter values P_j in both formats, $\alpha\lambda$ and α/ν^2.

As will be discussed below, the Ferrell−Bhattacharjee spectral function[24] applies to the measured spectra. This function involves an integral (eq 18) that has been calculated at 900 points using the Romberg method[55] and has been interpolated between these points.

3. C_6E_3/H_2O Mixtures

Triethylene glycol monohexyl ether (C_6E_3) has been purchased from Bachem Biochemica (Heidelberg, Germany). The

TABLE 1: Mole Fraction x, Mass Fraction Y, and Molar Concentration c of Surfactant as Well as Density ρ, Static Shear Viscosity η_s, and Sound Velocity c_s at Temperature T Displayed for the C_6E_3/H_2O Mixtures (Critical Temperature T_{crit} = (46.0 ± 0.04) °C)

x, 10^{-2}, ±0.2%	Y, 10^{-2}, ±0.1%	c, mol/L, ±0.2%	T, °C	ρ, g/cm^3, ±0.1%	η_s, 10^{-3} Pa·s, ±0.2%	c_s, m/s, 300 kHz, ±0.1%	c_s, m/s, 100 MHz, ±0.05%
0.157	2.0	0.085	17.5	1.000	1.160	1493.2	1493.3
			25.0	0.999	0.966	1506.9	1511.9
			32.5	0.997	0.822	1528.3	1526.3
			40.0	0.994	0.706	1539.9	
0.403	5.0	0.213	17.5	1.000	1.342	1495.8	1500.2
			25.0	0.999	1.118	1503.2	1511.5
			32.5	0.997	0.954	1523.1	1525.8
			40.0	0.994	0.829	1531.6	
0.664	8.0	0.341	17.5	1.000	1.605	1496.8	1507.0
			25.0	0.998	1.332	1500.5	1516.9
			32.5	0.995	1.152	1513.8	1526.5
			40.0	0.993	1.026	1523.0	
0.941	11.0	0.469	17.5	1.001	1.942	1497.7	1508.0
			25.0	0.999	1.600	1500.1	1514.4
			32.5	0.996	1.392	1510.1	1521.5
			40.0	0.993	1.255	1518.6	
1.300	14.6	0.623	17.5	0.997	2.365	1493.8	1590.2
			25.0	0.996	1.951	1501.4	1516.5
			32.5	0.992	1.676	1505.7	1520.8
			40.0	0.988	1.477	1510.3	

compound was claimed to be 98% pure. It was used as delivered. Water was deionized by mixed-bed ion exchange, additionally distilled twice, and UV-sterilized. The C_6E_3/H_2O mixtures were prepared by weighing appropriate amounts of the surfactant into suitable flasks, which were filled up to the line measure with water. The density ρ of the mixtures has been measured pycnometrically. The (static) shear viscosity η_s of the sample liquids has been determined with a falling-ball viscometer (Haake, Berlin, Germany). A survey of the solutions and a compilation of the ρ, η_s, and c_s data at the temperatures of measurement is given in Table 1.

Because of the strong dependence of the critical temperature T_{crit} upon small amounts of impurities, the T_{crit} of the actual mixture of critical composition has been measured to within ±0.04 K by monitoring the light from a He−Ne laser scattered by the sample. Increasing slowly the temperature we found T_{crit} = 46.0 °C, which is rather close to the literature value (44.7 °C[34]). During a series of ultrasonic measurements, we did not find indications of a noticeable variation of T_{crit}, as had been reported by Zielesny et al.[7]

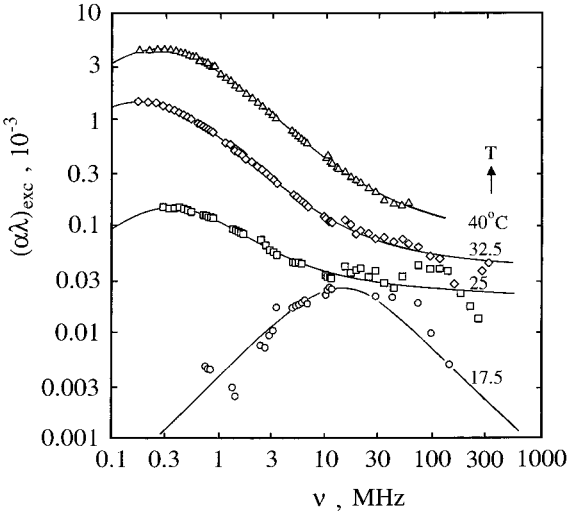

Figure 1. Ultrasonic excess absorption spectra for the C_6E_3/water mixture with mass fraction $Y = 0.02$ of surfactant at four temperatures T. The full lines represent a Debye term (17.5 °C, eq 13) and the sum of a restricted Hill term and a Bhattacharjee-Ferrell term (T > 17.5 °C, eq 21) with the parameter values given in Table 2.

4. Results and Discussion

Premicellar Absorption (c < cmc); Monomer Exchange (c ≥ cmc). In Figure 1 excess absorption spectra of the 0.085 M solution (Y = 0.02) are displayed at four temperatures T. When T is raised from 17.5 to 25 °C the cmc of the system is passed over.[16] This crossing of the cmc is clearly indicated by the sonic spectra. Particularly at low frequencies (ν < 3 MHz), additionally strong contributions to the absorption per wavelength arise if the surfactant concentration exceeds the cmc.

It is interesting to notice that, in conformity with previous results for *n*-heptylammonium chloride aqueous solutions,[56] there already exists excess absorption at c < cmc where only oligomeric species might be present. Since the cmc is comparatively small here, the amplitude of the excess absorption spectrum at c < cmc is likewise small so that a considerable error in the $(\alpha\lambda)_{exc}$ values results. It is thus impossible to analyze the shape of the excess absorption in terms of specific relaxation spectral functions. For this reason the spectrum at 17.5 °C has been analytically represented assuming a simple Debye function with discrete relaxation time τ_D.[57] Hence the spectral function

$$R_D(\nu) = \frac{A_D \omega \tau_D}{1 + (\omega \tau_D)^2} + B\nu \qquad (13)$$

has been used. Herein, $\omega = 2\pi\nu$ and A_D is the relaxation amplitude.

In the case of *n*-heptylammonium chloride aqueous solutions, at concentrations slightly above the cmc,[56] the Hill relaxation spectral function[58−60] turned out to apply to the low-frequency part of the spectrum (ν < 100 MHz). This function, given by

$$R_H(\nu) = \frac{A_H (\omega \tau_H)^{m_H}}{(1 + (\omega \tau_H)^{2s_H})^{(m_H + n_H)/(2s_H)}} + B\nu \qquad (14)$$

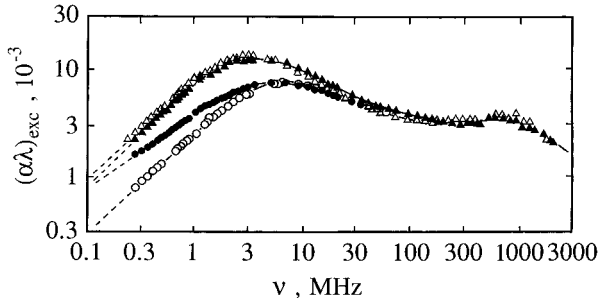

Figure 2. Ultrasonic excess absorption spectra for the C_6E_3/water mixture with mass fraction $Y = 0.08$ of surfactant at 17.5 °C (▲) and 40 °C (●) and for a C_6E_4/water mixture of the same mass fraction at 17.5 °C (△) and 40 °C (○).

is based on a continuous relaxation time distribution function $G_H(\ln(\tau/\tau_H))$. Parameters m_H, n_H, s_H ($0 < m_H, n_H, s_H \leq 1$) determine the width and shape of G_H. The Hill spectral function R_H has been attributed to the monomer exchange process.[56] As compared to "proper" micelle systems, at surfactant concentrations distinctly above the cmc somewhat modified kinetics have been assumed[6] in order to allow for the distribution of relaxation times in the *n*-heptylammonium chloride/water spectra. With the C_6E_3/water system, however, even the Hill relaxation spectral function (eq 14) cannot adequately account for the high-frequency wing in the excess absorption spectrum at $c >$ cmc (Figure 1). In addition to the contribution that is due to the kinetics of micelle formation and decay, there seems to exist a broad-band background contribution as characteristic for critical systems.[32,61−64]

Critical Absorption. The spectra shown in Figure 1 are dominated by the absorption mechanism related to the micelle kinetics. These spectra thus do not allow for an easy extraction of the background contribution. In Figure 2, therefore, results for a C_6E_3/water mixture ($Y = 0.08$) at two different temperatures are compared to those for a C_6E_3/water mixture with the same mass fraction of surfactant. Both surfactant systems differ from another especially by the critical temperature, which is substantially higher with C_6E_4/H_2O ($T_{crit} = 66.3$ °C) than with C_6E_3/H_2O ($T_{crit} = 46$ °C). At 17.5 °C nearly identical spectra for both C_iE_j/water systems point at almost identical micelle formation/decay kinetics in the surfactant solutions. At 40 °C, however, where the C_6E_3/H_2O mixture is substantially closer to its demixing temperature than the C_6E_4/H_2O mixture, the former exhibits distinctly higher excess absorption at low frequencies than the latter ($(\alpha\lambda)_{exc} = 0.8 \times 10^{-3}$, C_6E_4; $(\alpha\lambda)_{exc} = 1.6 \times 10^{-3}$, C_6E_3; 300 kHz).

These characteristics in the ultrasonic spectra of the two systems at different temperatures may be taken as a first indication of the existence of a critical part in the absorption coefficient of the micellar systems. Another remarkable result from the ultrasonic absorption spectra is the finding of the critical and noncritical contributions to obviously not simply superimpose. In the case of a linear superposition, the low-frequency (relative) maximum of the C_6E_3/H_2O spectrum at 40 °C should exceed that of the C_6E_4/H_2O system at the same temperature.

During the past years, the Bhattacharjee-Ferrell model,[24,27,65,66] which is based on the dynamic scaling hypothesis,[67,68] has proven a satisfactory description of the sonic excess absorption of various binary liquids with miscibility gap.[32] The Bhattacharjee−Ferrell spectral function R_{BF} may be expressed as

$$R_{BF}(\nu) = A_{BF}\omega^{-\tilde{\alpha}/(z\tilde{\nu})}F(\Omega) \qquad (15)$$

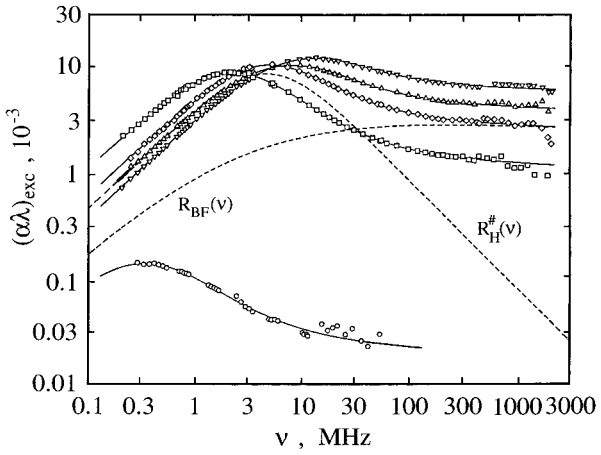

Figure 3. Ultrasonic excess absorption spectra at 25 °C for the C_6E_3/water mixtures with mass fraction $Y = 0.02$ (○), $= 0.05$ (□), $= 0.08$ (◇), $= 0.11$ (△), and $= 0.146$ (▽). Dashed curves are graphs of the restricted Hill term (eq 20) and the Bhattacharjee−Ferrell term (eq 15) of the $Y = 0.08$ spectrum. Full curves show the sum of these terms with the parameter values obtained from the fitting procedure (Table 2).

where the amplitude A_{BF} is given by

$$A_{BF} = \hat{A}_{BF}\frac{\pi\tilde{\alpha}}{2z\tilde{\nu}}\omega_0^{\tilde{\alpha}/(z\nu)} \qquad (16)$$

Herein $\tilde{\alpha}$ and $\tilde{\nu}$ are the critical exponents for the specific heat capacity and the fluctuation correlation length ξ, respectively, and z is the dynamical critical exponent. $\Omega = \omega/\omega_D$ is the reduced frequency with

$$\omega_D = 2D/\xi^2 = \omega_0 t^{z\tilde{\nu}} \qquad (17)$$

D denotes the mutual diffusion coefficient, ω_0 is the characteristic angular frequency of fluctuations, and $t = |T - T_{crit}|/T_{crit}$ is the reduced temperature. In eq 15 the scaling function F is given by the integral

$$F(\Omega) = \frac{3}{\pi}\int_0^\infty \frac{x^2}{(1+x^2)^2}\frac{K_{BF}(x)}{K^2{}_{BF}(x) + \Omega^2}\,dx \qquad (18)$$

where

$$K_{BF}(x) = x^2(1+x^2)^p \qquad (19)$$

and $p \approx 0.5$ for three-dimensional systems. Bhattacharjee and Ferrell have also presented other versions of the scaling function. However, the integral as defined by eqs 18 and 19 largely agrees with the Kroll and Ruhland scaling function[69,70] and is thus preferred here.

Model Relaxation Spectral Function. In view of the characteristics of the measured spectra, a sum of a Hill term and a Bhattacharjee−Ferrell term appears to be appropriate to analytically represent the frequency-dependent ultrasonic excess absorption (Figure 3). It turned out, however, that the relaxation time distribution parameters m_H and n_H in the Hill term can be fixed at $m_H = n_H = 1$. Hence the reduced Hill relaxation term

$$R^{\#}_H(\nu) = 2^{1/s_H - 1}A^{\#}_H\frac{\omega\tau_H}{(1+(\omega\tau_H)^{2s_H})^{1/s_H}} \qquad (20)$$

allows for an adequate representation of the micelle kinetics contribution. In this spectral term $A^{\#}_H = 2R^{\#}_H(\nu = (2\pi\tau_H)^{-1})$ as

TABLE 2: Parameter Values of the Model Relaxation Spectral Function $R_m(\nu)$ As Obtained from the Nonlinear Least-Squares Regression Analysis of the Ultrasonic Absorption Spectra for C_6E_3/H_2O Mixtures at Different Temperatures T

Y, 10^{-2}	T, °C	$A_H^{\#}$, 10^{-3}, ±10%	τ_h, ns, ±5%	s_H, ±5%	A_{BF}, 10^{-3}, ±5%	ω_D, 10^6 s^{-1}, ±10%	B, 10^{-12} s, ±0.5%
2.0	17.5	0.005	11	1			41.40
	25.0	0.245	447	0.77	0.079	0.1	32.88
	32.5	2.77	909	0.65	0.148	0.1	26.79
	40.0	8.85	602	0.68	0.296	0.1	22.92
5.0	17.5	20.0	106	0.82	4.0	2.4	43.34
	25.0	16.2	78	0.75	4.9	12.5	34.27
	32.5	13.0	65	0.85	4.7	3.5	28.35
	40.0	10.9	64	0.87	4.9	1.6	26.0
8.0	17.5	21.5	44	0.81	10.4	12	45.46
	25.0	16.9	36	0.84	10.4	11	36.62
	32.5	13.1	32	0.68	9.9	11	30.43
	40.0	9.7	31	0.75	10.8	3.8	27.0
11.0	17.5	21.4	29	0.77	16.0	17	49.01
	25.0	15.5	24	0.69	15.7	18	38.89
	32.5	12.9	22	0.52	14.9	27	33.32
	40.0	7.6	23	0.65	14.4	4.0	30.0
14.6	17.5	23.8	19	0.66	27.7	61	51.48
	25.0	17.1	16	0.63	23.6	39	41.05
	32.5	11.6	14	0.67	21.8	16	35.45
	40.0	9.3	10	0.65	16.4	4.8	32.0

with a Debye relaxation spectral term that follows from eq 20 at $s_H = 1$. Finally the model function

$$R_m(\nu) = R_H^{\#}(\nu) + R_{BF}(\nu) + B\nu \tag{21}$$

has been fitted to the measured $\alpha\lambda$ vs ν relations. The values of the parameters of $R_m(\nu)$, as following from the nonlinear least-squares regression analysis of the absorption data, are displayed in Table 2.

Kinetics of Micelle Formation. The relaxation rates τ_H^{-1} of the low-frequency Hill relaxation term (Table 2) largely follow the Teubner−Kahlweit theory[22,23] which, based on the reaction scheme given in eq 1, predicts

$$\tau_H^{-1} = k^b\left(\frac{1}{\sigma^2} + \frac{X}{\bar{m}}\right) \tag{22}$$

where

$$X = (c - c_1)/c_1 \approx (c - \text{cmc})/\text{cmc} \tag{23}$$

In deriving eq 22 a Gaussian distribution

$$(k_{i+1}^b \bar{N}_{i+1} - k_i^b \bar{N}_i)/\bar{N}_i = k^b/\sigma^2(i - \bar{m}) \tag{24}$$

of micelle sizes around the mean aggregation number $\bar{m}$ is assumed. Here σ^2 is the variance of the distribution function, and the $\bar{N}_i$ denote the molar concentrations at thermal equilibrium. $k^b(= k_{\bar{m}}^b)$ is the backward reaction rate corresponding with the maximum of the distribution function. Around this maximum $k_i^b \approx k_{i+1}^b$ is assumed. Deviations from the linear dependence of the relaxation rate τ_H^{-1} upon X emerge at 17.5 °C and, to somewhat smaller extend, also at 25 °C where, near the cmc, the τ_H^{-1} values increase toward smaller solute concentration. In Figure 4 this noteworthy behavior is illustrated by the τ_H^{-1} data at 17.5 °C. Also presented in this diagram are relaxation rate data for aqueous solutions of heptylammonium chloride solutions to show that a similar effect results for ionic surfactants with small hydrocarbon chain.[56,71] It has been also reported by other scientists.[16,17,72] Qualitatively, an increase in τ_H^{-1} with decreasing c at $c \approx$ cmc is predicted by an extended model of stepwise association[6] and is attributed to the premicellar formation of oligomeric aggregates.

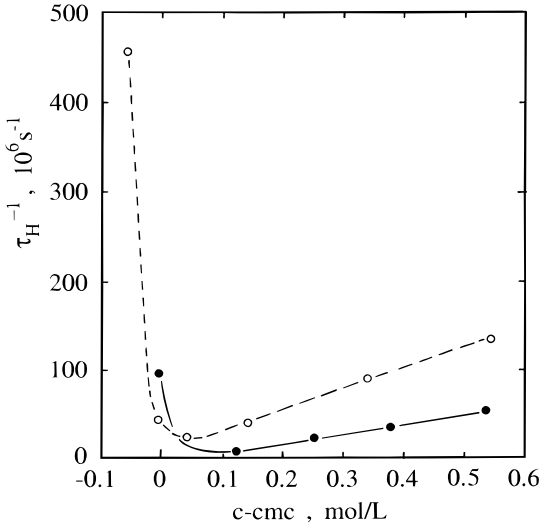

Figure 4. Relaxation rate τ_H^{-1} of the restricted Hill term displayed versus the concentration difference c − cmc for the C_6E_3/water mixtures at 17.5 °C (●) and for aqueous solutions of *n*-heptylammonium chloride at 25 °C (○), refs 56 and 71, cmc ≈ 0.45 mol/L).

At 32.5 and 40 °C the τ_H^{-1} vs X relation shows deviations from linearity toward higher solute concentrations. The tendency of the τ_H^{-1} data at $c > 0.5$ mol/L to exceed the predictions from eq 22, however, may, at least in part reflect the uncertainty in the relaxation time values at these high concentrations due to the strong masking of the Hill-type relaxation by the concentration fluctuation contributions to the sonic spectra.

According to eq 22 the linear part in the τ_H^{-1} vs X relation allows one to determine the ratio $k^b/\bar{m}$. Using, in addition, $\bar{m}$ and cmc values as obtained by interpolation of literature data,[35,73] the k^b and $k^f = k^b/\text{cmc}$[22,23] values displayed in Table 3 have been derived. Here k^f denotes the forward rate constant corresponding to the maximum in the distribution function ($k^f = k_{\bar{m}}^f$), also nearly constant at $i \approx \bar{m}$. Both k^b and k^f are only weakly dependent upon temperature. The small increase in k^f with T may result from an enhancement of the mobility of monomers owing to the decreasing viscosity of the suspending phase. A noteworthy result is the missing of any tendency in the parameter values that could be taken to suggest a growth of the mean aggregation number on approaching the critical

TABLE 3: Values of the Critical Micelle Concentration cmc and the Mean Aggregation Number $\bar{m}$ as Obtained from Interpolation of Literature Data[35,73] as Well as Reaction Rate Data and Reaction Volumes of the Isodesmic Reaction Scheme (Eq 1) of Micelle Formation as Following from the Restricted Hill Relaxation Spectral Term

T, °C	cmc, 10^{-3} mol/L	$\bar{m}$	k^b, 10^9 s^{-1}	k^f, 10^9 s^{-1} mol/L^{-1}	ΔV, cm^3/mol
17.5	98	57	0.58	5.9	8.8
25.0	92	57	0.59	6.4	7.8
32.5	86	57	0.57	6.7	7.2
40.0	82	57	0.55	6.8	6.6

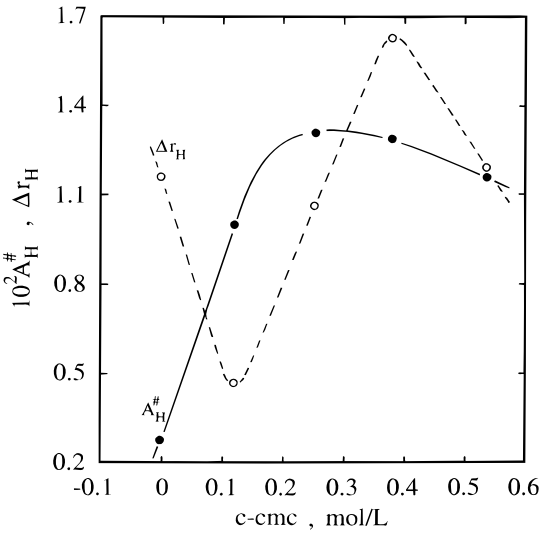

Figure 5. Amplitude $A_H^\#$ and half-maximum bandwidth Δr_H of the relaxation time distribution function (Figure 6) displayed as a function of c − cmc for the C_6E_3/water mixtures at 32.5 °C.

concentration c_{crit} and temperature T_{crit}. This finding is another indication for the soundness of the assumption that small C_6E_3 micelles continue to exist also near the critical point of the system.

As shown by Figure 5 the relaxation amplitudes $A_H^\#$ of the restricted Hill term are also largely in conformity with the Teubner−Kahlweit model, which predicts

$$A_H^\# = \frac{\pi(\Delta V)^2 \mathrm{cmc}}{\kappa_s^\infty RT} \frac{(\sigma^2/\bar{m})X}{1+(\sigma^2/\bar{m})X} = \frac{\pi(\Delta V)^2 \mathrm{cmc}}{\kappa_s^\infty RT} \frac{c-\mathrm{cmc}}{(\bar{m})\mathrm{cmc}/\sigma^2 + c - \mathrm{cmc}} \quad (25)$$

Here ΔV is the reaction volume, which is assumed[22,23] to be the same ($\Delta V = \Delta V_i$, i = 2, 3, ...) in all steps of coupled reactions (eq 1), κ_s^∞ is the adiabatic compressibility extrapolated to high frequencies, and R is the gas constant. At c − cmc < 0.15 mol/L, the $A_H^\#$ values increase substantially with surfactant concentration to nearly reach a plateau at high solute content. At 32.5 °C, the $A_H^\#$ value at the highest surfactant concentration (0.623 mol/L) is somewhat smaller than at 0.341 and 0.469 mol/L (Figure 5). Even this deviation, however, scarcely exceeds the limits of experimental error. We thus used the mean of the nearly constant amplitudes at higher concentrations (c − cmc > 0.2 mol/L) to define a maximum value $A_H^\#$ and to calculate according to

$$\Delta V = \left(\frac{A_{H\max}^\# \kappa_s^\infty RT}{\pi \mathrm{cmc}}\right)^{1/2} \quad (26)$$

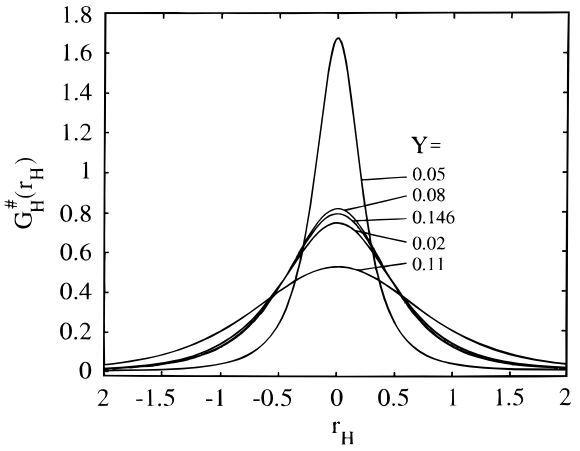

Figure 6. Plot of the relaxation time distribution function $G_H^\#(r_H)$ of the restricted Hill term (eq 30) for C_6E_3/water mixtures at 32.5 °C and at different mass fractions Y of surfactant.

the reaction volume as a function of temperature. The ΔV values resulting from this evaluation of relaxation amplitude data are also collected in Table 3.

The reaction volume, essentially the difference in the molar volume of monomers in solution and within micelles, decreases with temperature. This is likely an effect of hydration. The voluminous clathrate-like hydrogen-bonded water structure around the nonionic surfactant molecules is gradually broken with increasing temperature, when the water properties and structure tend to approach those of a normal liquid.

Another interesting characteristic of the low-frequency spectral term is its width as reflected by the s_H-parameter of the restricted Hill function. Let us ignore the premicellar system (Y = 0.02, 17.5 °C), the small relaxation amplitude of which ($A_H^\# = 5 \times 10^{-6}$) prevents the excess absorption spectrum from being analyzed in terms of its particular shape. The relaxation time distribution parameter values of the other solutions ($0.52 \le s_H \le 0.87$, Table 2) exhibit considerable deviations from a Debye-type relaxation behavior for which $s_H \equiv 1$. In Figure 6 these deviations are illustrated by a plot of the relaxation time distribution function $G_H^\#(r_H) = G_H^\#(\ln(\tau/\tau_H))$ for the C_6E_3 solutions at 32.5 °C. The distribution function $G_H^\#(r_H)$ corresponding to the restricted Hill spectral term $R_H^\#(\nu)$ is defined by

$$R_H^\#(\nu) = A_H^\# \int_0^\infty G_H^\#(r_H) \frac{\omega\tau}{1+\omega^2\tau^2} \, dr_H \quad (27)$$

with

$$\int_0^\infty G_H^\#(r_H) \, dr_H = 1 \quad (28)$$

and

$$r_H = \ln(\tau/\tau_H) \quad (29)$$

The graphs shown in Figure 6 have been calculated by analytical continuation[74] of the relation

$$G_H^\#(r_H) = \frac{2}{\pi} \hat{G}_H^\# Re\left\{\frac{-ie^{-r_H}}{(1+(-ie^{r_H})^{2s_H})^{(1/s_H)}}\right\} \quad (30)$$

The amplitude parameter $\hat{G}_H^\#$ follows from normalization using eq 28.

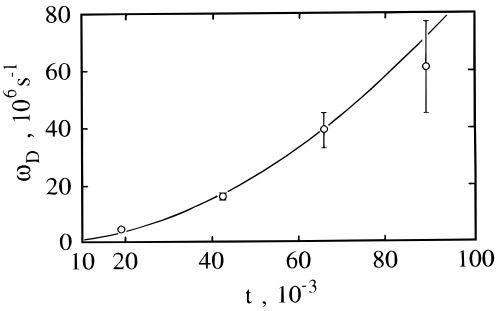

Figure 7. Relaxation rate of fluctuations ω_D of the Bhattacharjee−Ferrell model (symbols, Table 2) versus reduced temperature t for the C_6E_3/water mixture of critical composition ($Y = 0.146$). The full line shows the predictions from eq 17 with the diffusion coefficient estimated from our viscosity data.

The half-maximum bandwidths Δr_H of the symmetrically shaped relaxation time distribution functions at 32.5 °C are shown in Figure 5. In conformity with the results for the system *n*-heptylammonium chloride/water,[56] the distribution function is rather broad at $c \approx$ cmc. Near the critical micelle concentration, where oligomeric structures are formed instead of proper micelles, nonvanishing Δr_H values are also predicted by the extended Teubner−Kahlweit model.[6] For solute concentrations distinctly above the cmc, however, the theoretical model yields an almost Debye-type relaxation behavior, and small relaxation time distribution functions have in fact been found with the aqueous solutions of *n*-heptylammonium chloride.[56] With the nonionic C_6E_3 aqueous solutions noteworthy high Δr_H values at $c -$ cmc > 0.2 mol/L, where $\Delta r_H > 1$ (Figure 5), may be taken to be due to local fluctuations in the micelle concentration. According to eq 22, the relaxation rate τ_H^{-1} depends on the (local) surfactant concentration. Hence fluctuations in the concentration will also lead to local variations in the relaxation rate as reflected by a relaxation time distribution. Another reason for deviations from a single-Debye-term behavior at high surfactant content may be a deformation of the micelles leading to nonglobular shapes. Different curvatures along the surface of nonspherically shaped micelles may result in spatial variations of the rate constants for the monomer exchange at the micellar surface and may thus also be the cause of a distribution of relaxation rates.

Critical Fluctuations of Micelle Concentration. For the mixture of critical composition, the parameters of the R_{BF} term in the model relaxation spectral function (eq 21) may be considered in terms of the Bhattacharjee−Ferrell theory of sonic absorption. The theoretical model predicts the characteristic angular frequency (eq 17)

$$\omega_0 = k_B T/(3\pi\eta_0\xi_0^3) \tag{31}$$

to be given by the amplitudes η_0 and ξ_0 of the shear viscosity η_s and correlation length ξ, respectively. The viscosity amplitude is defined by the relation

$$\eta_s(T) = \eta_0 t^{-(z-3)\tilde{\nu}} \tag{32}$$

and ξ_0 by eq 2. In eq 31 k_B denotes Boltzmann's constant. In eqs 31 and 32 the viscosity is treated without considering a background contribution, which is clearly a simplification. Using eq 32 just to interpolate our viscosity data (Table 1) and taking $\xi_0 = 0.35$ nm,[7] $\omega_0 = 7.4 \times 10^9$ s^{-1} follows at T_{crit}. Assuming ω_0 independent of temperature, the t dependence of ω_D (eq 17) as displayed in Figure 7 results. As also illustrated by that diagram these ω_D values nicely agree with the data from the ultrasonic absorption spectra. This is a remarkable result since the agreement between the values calculated from eqs 17 and 31 on one hand and from the relaxation behavior of the mixture of critical composition on the other hand exists without any adjustment of parameters. Hence the conclusion may be drawn that the molecular dynamics behind the R_{BF} term of the model relaxation spectral function obeys the dynamic scaling hypothesis.

The amplitude $\hat{A}_{BF}$ (eq 16) of the Bhattacharjee−Ferrell term in the model relaxation spectral function (eq 21) according to[26,28]

$$\hat{A}_{BF} = \frac{\pi g^2 c_s \tilde{A}}{T\tilde{B}^2} \tag{33}$$

is related to the critical contribution $\tilde{A}$ and the background part $\tilde{B}$ of the specific heat at constant pressure

$$c_p = \tilde{A}t^{-\tilde{\alpha}} + \tilde{B} \tag{34}$$

In eq 33 the coupling constant g is given by[75]

$$g = -\rho_{cr}c_p\left(\frac{dT_c}{dp} - \frac{T\alpha_p}{\rho c_p}\right) = \tilde{B}\tilde{C}_0 T_c/\tilde{A} - \tilde{C}_1 T \tag{35}$$

where ρ_{cr} is the density of the system at the critical point and

$$\alpha_p = \tilde{C}_0\tilde{t}^{-\tilde{\alpha}} + C_1 \tag{36}$$

is the thermal expansion coefficient. Because there do not seem to exist experimental data for the critical part $\tilde{A}$ in the specific heat, we used the relation

$$\left(\frac{\tilde{\alpha}\tilde{A}\rho_{cr}}{k_B}\right)^{1/3}\xi_0 = R_\xi^+ = 0.27 \tag{37}$$

to calculate $\tilde{A}$ from known ξ_0 and ρ_{cr} data. Relation 37 follows from the two-scale-factor universality concept[77] that has been verified by results for several binary mixtures.[75,76,78,79] Taking $\tilde{B} = 4185$ J·kg^{-1} K^{-1}, which is the heat capacity of liquid water at room temperature, with $\tilde{A} = 57.6$ J·kg^{-1} K^{-1} (eq 37), according to eq 33 $g = 0.81$ follows from $\hat{A}_{BF}$. The value obtained for the coupling constant is quite reasonable, particularly because similar values have been found for other binary mixtures.[80,81] The verification by independent methods of the g-value for the C_6E_3/H_2O system, however, is still necessary.

Noncritical Concentration Fluctuations. The Bhattacharjee−Ferrell term $R_{BF}(\nu)$ in the model relaxation spectral function (eq 21) is based on the idea of fluctuations that span a broad regime of correlation lengths. Rather surprisingly, this term applies also to the spectra for mixtures of noncritical concentrations. Only the ω_D data for the mixture of critical composition, however, show the theoretically predicted behavior (eq 17, Figure 7). The ω_D values for the other mixtures are almost independent of temperature. These unexpected characteristics in ω_D may be due to contrary effects. In the noncritical mixtures the "normal" reduction in ω_D when T_c is approached (eq 17) may be compensated by a simultaneous enhancement of the correlation length. This idea is in conformity with the appearance of small droplets in noncritical mixtures at their phase separation temperature, whereas critical systems exhibit schlieren only. Such observations have been reported for the isobutoxyethanol/water system[49] and also for mixtures of nitrobenzene and isooctane.[82] In conformity with the ω_D values,

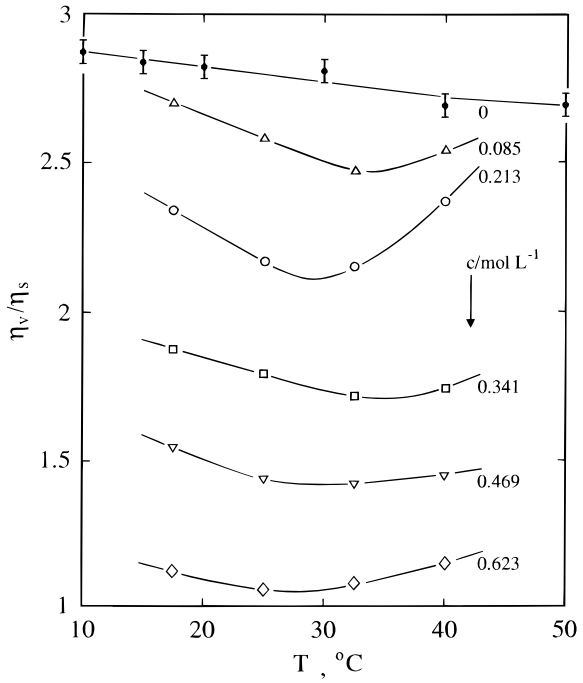

Figure 8. Volume viscosity to shear viscosity ratio η_v/η_s (eq 38) for water (●) and for the C_6E_3/water mixtures of different surfactant concentration plotted versus temperature *T*. The water data have been calculated using c_s values from Bilaniuk and Wong,[40] *B*-values from this laboratory, and density and shear viscosity data according to Kell.[41]

the amplitudes for the BF term of noncritical composition also do not show a noticeable dependence upon temperature (Table 2).

Volume Viscosity; Adiabatic Compressibility. As reflected by the *B* values (Table 2), the asymptotic high-frequency part in the ultrasonic spectra of the C_6E_3/water mixtures shows the normal behavior. At each temperature of measurement *B* increases monotonically with surfactant concentration. For aqueous mixtures, for which the heat conductivity contribution to the high-frequency sonic absorption is negligibly small,[83,84] *B* depends linearly upon the shear viscosity η_s and the volume viscosity, η_v. Hence it is possible to calculate the viscosity ratio

$$\frac{\eta_v}{\eta_s} = B\frac{c_s^2\rho}{2\pi^2\eta_s} - \frac{4}{3} \qquad (38)$$

from the *B* and η_s data. Theoretical considerations yield $\eta_v/\eta_s = 2/3$[85,86] for liquids without relaxation process at frequencies above the measuring range. For water, however, considerably higher viscosity ratios are found ($\eta_v/\eta_s = 2.68$, 25 °C[87]). These high values have been taken as an indication of the existence of a high-frequency structure relaxation in the hydrogen-bonded water network. Solutes tend to disturb the water structure and to thus give rise to η_v/η_s values smaller than those of the associating solvent. The viscosity ratio of the C_6E_3/water mixtures in fact decreases monotonically with surfactant concentration (Figure 8). At least at low solute content, however, a relative minimum emerges in the η_v/η_s vs *T* relation, an effect that presently cannot be unambiguously explained.

A relative minimum results also when the adiabatic compressibility

$$\kappa_s = \rho^{-1}c_s^{-2} \qquad (39)$$

of the C_6E_3/water mixtures at temperature *T* is plotted as a function of surfactant concentration (Figure 9). The reduction in κ_s when the solute is added to water again reflects the disturbance of the voluminous hydrogen-bonded water network of high compressibility ($\kappa_s = 4.479 \times 10^{-10}$ m^2 N^{-1}, water 25 °C). At $T \geq 25$ °C the adiabatic compressibility increases with *c*, indicating that in more concentrated solutions again highly compressible structures are formed. This is particularly true at higher temperatures (32.5, 40 °C) where the effect of the hydrogen network in the water properties is already somewhat reduced.

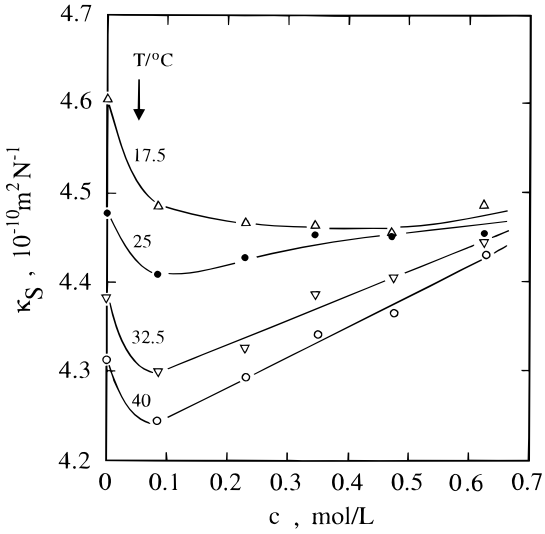

Figure 9. Adiabatic compressibility κ_s (eq 39) of the C_6E_3/water system shown as a function of surfactant concentration *c*. The values for water have been calculated using c_s and ρ data from the literature.[40,41]

5. Conclusions

The broad-band ultrasonic absorption measurements of the C_6E_3/water system as a function of composition and temperature confirm previous results for aqueous solutions of the cationic surfactant *n*-heptylammonium chloride[56] inasmuch as the formation of oligomeric species at concentrations smaller than, or about equal to, the cmc is clearly reflected by the sonic spectra. At surfactant concentration *c* well above the cmc, the amplitude and relaxation time of the ultrasonic relaxation process, which is related to the monomer exchange between micelles and the suspending liquid, follows the predictions of the Teubner−Kahlweit theory.[22,23] Only close to the cmc the relaxation rate increases at decreasing *c*. This behavior is assumed to be due to the formation of micelles from oligomeric species. In contrast to the Teubner−Kahlweit model, the monomer exchange relaxation term is subject to a relaxation term distribution that seems to predominantly result from fluctuations in the local concentration and thus in the relaxation rate.

In excess of the absorption due to the monomer exchange, there exists also a critical contribution to the ultrasonic spectra of the C_6E_3/water mixtures of critical composition. The Bhattacharjee−Ferrell model[24,65] is sufficient here to describe these contributions, since their amplitude is small as compared to that from the micelle kinetics. It is thus not necessary to use more recent theoretical approaches[89−93] in order to appropriately describe the measured ultrasonic spectra. This is in particular true because the values for the relaxation rate ω_D of local energy fluctuations as derived from (static) viscosity data nicely agree with those extracted from our spectra. Also reasonable is the value of the coupling constant ($g = 0.81$). Unfortunately, *g*-values from independent experimental methods are missing.

We interpret the critical contribution to the sonic spectra to reflect fluctuations of the concentration of complete micelles. However, further studies are necessary and are currently in progress[94] to reach a definite conclusion on the mechanisms underlying the dynamics of the C_6E_3/water mixtures.

The Bhattacharjee−Ferrell relaxation spectral function applies also to the spectra for the C_6E_3/water mixtures of noncritical composition. The ω_D values obtained for those mixtures, however, do not follow the predictions for a critical system.

Acknowledgment. We thank Drs. S. Z. Mirzaev and A. Rupprecht for helpful discussions and Mrs. N. Jehrke for the viscosity measurements. Financial assistance by the Deutsche Forschungsgemeinschaft is gratefully acknowledged.

References and Notes

(1) Aniansson, E. A. G.; Wall, S. N. *J. Phys. Chem.* **1974**, *78*, 1024.
(2) Aniansson, E. A. G.; Wall, S. N. *J. Phys. Chem.* **1975**, *79*, 857.
(3) Aniansson, E. A. G. *J. Phys. Chem.* **1978**, *82*, 2805.
(4) Aniansson, E. A. G. *Ber. Bunsen-Ges. Phys. Chem.* **1978**, *82*, 981.
(5) Aniansson, E. A. G. *Prog. Colloid Polym. Sci.* **1985**, *70*, 2.
(6) Telgmann, T.; Kaatze, U. *J. Phys. Chem. B* **1997**, *101*, 7766.
(7) Zielesny, A.; Belkoura, L.; Woermann, D. *Ber. Bunsen-Ges. Phys. Chem.* **1994**, *98*, 579.
(8) Corti, M.; Degiorgio, V. *J. Chem. Phys.* **1981**, *85*, 1442.
(9) Hamano, K.; Yamashita, S.; Sengers, J. V. *Phys. Rev. Lett.* **1992**, *68*, 3579.
(10) Gormally, J.; Gettins, W. J.; Wyn-Jones, E. In *Molecular Interactions*; Ratajezak, H., Orville-Thomas, W., Eds.; Wiley: Chichester, 1981; Vol. 2, p 143.
(11) Gharibi, H.; Takisawa, N.; Broun, P.; Thomasson, M. A.; Painter, D. M.; Bloor, D. M.; Hall, D. G.; Wyn-Jones, E. *J. Chem. Soc., Faraday Trans. 1* **1991**, *87*, 707.
(12) Wan-Bahdi, W.; Palepu, R.; Bloor, D. M.; Hall, D. G.; Wyn-Jones, E. *J. Phys. Chem.* **1991**, *95*, 6642.
(13) Thomasson, M. A.; Bloor, D. M.; Wyn-Jones, E. *J. Phys. Chem.* **1991**, *95*, 6017.
(14) Vicart, E.; Jobe, D. J.; Skalski, B.; Verrall, R. E. *J. Phys. Chem.* **1992**, *96*, 2348.
(15) Jobe, D. J.; Verrall, R. E.; Skalski, B.; Vicart, E. *J. Phys. Chem.* **1992**, *96*, 6811.
(16) Frindi, M.; Michels, B.; Levy, H.; Zana, R. *Langmuir* **1994**, *10*, 1140.
(17) Frindi, M.; Michels, B.; Zana, R. *J. Phys. Chem.* **1994**, *98*, 6607.
(18) Verrall, R. E.; Jobe, D. J.; Aicart, E. *J. Mol. Liq.* **1995**, *65/66*, 195.
(19) Zana, R.; Levy, H.; Papoutsi, D.; Beinert, G. *Langmuir* **1995**, *11*, 3694.
(20) Aliev, A. E.; Saidov, A. A.; Khabibullaev, P. K.; Shinder, J. J. *Acoust. Phys.* **1996**, *42*, 279.
(21) Khabibullaev, P. K.; Saidov, A. A.; Chestkov, E. V. *Physics-Doklady* **1997**, *42*, 471.
(22) Teubner, M. *J. Phys. Chem.* **1979**, *83*, 2917.
(23) Kahlweit, M.; Teubner, M. *Adv. Colloid Interface Sci.* **1980**, *13*, 1.
(24) Bhattacharjee, J. K.; Ferrell, R. A. *Phys. Rev. A* **1981**, *24*, 1643.
(25) Tanaka, H.; Wada, Y.; Nakajima, H. *Chem. Phys.* **1982**, *68*, 223.
(26) Garland, C. W.; Sanchez, G. *J. Chem. Phys.* **1983**, *79*, 3090.
(27) Ferrell, R. A.; Bhattacharjee, J. K. *Phys. Rev. A* **1985**, *31*, 1788.
(28) Tanaka, H.; Wada, Y. *Phys. Rev. A* **1985**, *32*, 512.
(29) Tanaka, H.; Nishi, T.; Wada, Y. *Chem. Phys.* **1985**, *94*, 281.
(30) Anisimov, M. A. *Critical Phenomena in Liquids and Liquid Crystals*; Gordon and Breach: Philadelphia, PA, 1991.
(31) Menzel, K.; Rupprecht, A.; Kaatze, U. *J. Acoust. Soc. Am.* **1998**, *104*, 2741.
(32) Mirzaev, S. Z.; Telgmann, T.; Kaatze, U. *Phys. Rev. E*, in press.
(33) Degiorgio, V. In *Physics of Amphiphiles: Micelles, Vesicles and Microemulsions*; Degiorgio, V., Corti, M., Eds.; North-Holland: Amsterdam, 1985; p 303.
(34) Corti, M.; Minero, C.; Degiorgio, V. *J. Phys. Chem.* **1984**, *88*, 309.
(35) Borthakur, A.; Zana, R. *J. Phys. Chem.* **1987**, *91*, 5957.
(36) Frindi, M.; Michels, B.; Zana, R. *J. Phys. Chem.* **1992**, *96*, 6095.
(37) D'Arrigo, G.; Paparelli, A. *Phys. Rev. E* **1994**, *50*, 4817.
(38) Matheson, A. J. *Molecular Acoustics*; Wiley-Interscience: London, 1971.
(39) Eggers, F.; Kaatze, U. *Meas. Sci. Technol.* **1996**, *7*, 1.
(40) Bilaniuk, N.; Wong, G. S. K. *J. Acoust. Soc. Am.* **1993**, *93*, 1609.
(41) Kell, G. S. In *Water, A Comprehensive Treatise*; Franks, F., Ed.; Plenum: New York, 1972; Vol. 1, p 363.
(42) Kaatze, U.; Wehrmann, B.; Pottel, R. *J. Phys. E: Sci. Instrum.* **1987**, *20*, 1025.
(43) Eggers, F.; Kaatze, U.; Richmann, K. H.; Telgmann, T. *Meas. Sci. Technol.* **1994**, *5*, 1131.
(44) Labhardt, A.; Schwarz, G. *Ber. Bunsen-Ges. Phys. Chem.* **1976**, *80*, 83.
(45) Behrends, R.; Eggers, F.; Kaatze, U.; Telgmann, T. *Ultrasonics* **1996**, *34*, 59.
(46) Kononenko, V. S. *Sov. Phys. Acoust.* **1985**, *31*, 499.
(47) Kaatze, U.; Lautscham, K. *J. Phys. E: Sci. Instrum.* **1986**, *19*, 1046.
(48) Kaatze, U.; Kühnel, V.; Menzel, K.; Schwerdtfeger, S. *Meas. Sci. Technol.* **1993**, *4*, 1257.
(49) Menzel, K. Ph.D. Dissertation, Georg-August-University, Göttingen, 1993.
(50) Gailus, T. Ph.D. Dissertation, Georg-August-University, Göttingen, 1996.
(51) Kaatze, U.; Lautscham, K.; Brai, M. *J. Phys. E: Sci. Instrum.* **1988**, *21*, 98.
(52) Bömmel, H. E.; Dransfeld, K. *Phys. Rev. Lett.* **1958**, *1*, 234.
(53) Kaatze, U.; Kühnel, V.; Weiss, G. *Ultrasonics* **1996**, *34*, 51.
(54) Marquardt, D. W. *J. Soc. Indust. Appl. Math.* **1963**, *2*, 2.
(55) Press: W. H.; Teukolsky, S. A.; Vetterlin, W. T.; Flannery, B. P. *Numerical Recipes in C*; Cambridge University Press: Cambridge, 1992.
(56) Telgmann, T.; Kaatze, U. *J. Phys. Chem. B* **1997**, *101*, 7758.
(57) Debye, P. *Polare Molekeln*; Hirzel: Leipzig, 1929.
(58) Hill, R. M. *Nature (London)* **1978**, *275*, 96.
(59) Hill, R. M. *Phys. Status Solidi B* **1981**, *103*, 319.
(60) Menzel, K.; Rupprecht, A.; Kaatze, U. *J. Acoust. Soc. Am.* **1998**, *104*, 2741.
(61) Anisimov, M. A.; Voronov, V. P.; Malishev, V. M.; Svadkovskii, V. V. *Zh. ETF Pis. Red.* **1973**, *18*, 224.
(62) Garland, C. W.; Sanchez, G. *J. Chem. Phys.* **1983**, *79*, 3090.
(63) Tanaka, H.; Wada, Y. *Phys. Rev. A* **1985**, *32*, 512.
(64) Dürr, U.; Mirzaev, S. Z.; Kaatze, U. *J. Phys. Chem.*, submitted.
(65) Ferrell, R. A.; Bhattacharjee, J. K. *Phys. Rev. E* **1981**, *24*, 4095.
(66) Bhattacharjee, J. K.; Ferrell, R. A. *Physics A* **1998**, *250*, 83.
(67) Kadanoff, L. P.; Swift, J. *Phys. Rev.* **1968**, *166*, 89.
(68) Halperin, B. I.; Hohenberg, P. C. *Phys. Rev.* **1969**, *177*, 952.
(69) Kroll, D. M.; Ruhland, J. M. *Phys. Lett.* **1980**, *80A*, 45.
(70) Kroll, D. M.; Ruhland, J. M. *Phys. Rev. A* **1981**, *23*, 371.
(71) Telgmann, T. Diploma Thesis, Georg-August-University, Göttingen, 1994.
(72) Hall, D. G.; Wyn-Jones, E. *J. Mol. Liq.* **1986**, *32*, 63.
(73) Pakusch, A. Ph.D. Dissertation, Georg-August-University, Göttingen, 1983.
(74) Giese, K. *Adv. Mol Relax. Processes* **1973**, *5*, 363.
(75) Fast, S. J.; Yun, S. S. *J. Acoust. Soc. Am.* **1988**, *83*, 1384.
(76) Belkoura, L.; Harnisch, F. P.; Kölchens, S.; Müller-Kischbaum, T.; Woermann, D. *Ber. Bunsen-Ges. Phys. Chem.* **1987**, *91*, 1036.
(77) Bervillier, C.; Godrèche, *Phys. Rev. B* **1980**, *21*, 5427.
(78) Zalczer, G.; Beyens, D. *J. Chem. Phys.* **1990**, *92*, 6747.
(79) Würz, U.; Grubic, M.; Woermann, D. *Ber. Bunsen-Ges. Phys. Chem.* **1992**, *96*, 1460.
(80) Binana-Limbelé, W.; Van Os, N. M.; Rupert, L. A. M.; Zana, R. *J. Coll. Interface Sci.* **1991**, *144*, 458.
(81) Schubert, K.-V.; Strey, R.; Kahlweit, M. *J. Colloid Interface Sci.* **1991**, *141*, 21.
(82) Zielesny, A.; Woermann, D. *J. Chem. Soc., Faraday Trans.* **1995**, *91*, 3889.
(83) Lamb, J. *Physical Acoustics*; Mason, W. P., Ed.; Academic Press: New York, 1965; Vol. 2, Part A, p 203.
(84) Bhatia, A. B. *Ultrasonic Absorption*; Oxford University Press: Oxford, 1967.
(85) Madigosky, W. M.; Warfield, R. W. *J. Chem. Phys.* **1983**, *78*, 1912.
(86) Madigosky, W. M.; Warfield, R. W. *Acustica* **1984**, *55*, 123.
(87) Kaatze, U.; Brai, M.; Scholle, F.-D.; Pottel, R. *J. Mol. Liq.* **1990**, *44*, 197.
(88) Kohlrausch, F. *Praktische Physik*; Hahn, D., Wagner, S., Eds.; Teubner: Stuttgart, 1986; Vol. 3.
(89) Onuki, A. *Phys. Rev. E* **1997**, *57*, 403.
(90) Onuki, A. *J. Phys. Soc. Jpn.* **1997**, *66*, 511.
(91) Folk, R.; Moser, G. *Phys. Rev. E* **1998**, *57*, 705.
(92) Folk, R.; Moser, G. *Phys. Rev. E* **1998**, *58*, 6246.
(93) Folk, R.; Moser, G. *Int. J. Thermophys.* **1998**, *19*, 1003.
(94) Telgmann, T.; Kaatze, U. *J. Phys. Chem.*, submitted.